Received: 7 March 2020 | Revised: 29 June 2020 | Accepted: 17 July 2020

DOI: 10.1002/psc.3279

RESEARCH ARTICLE

Journal of PeptideScience WILEY

# C-terminal tails mimicking bioactive intermediates cause different plasma degradation patterns and kinetics in neuropeptides γ-MSH, α-MSH, and neurotensin

Luana Palazzi[1] | Antonella Pasquato[2] | Mattia Vicario[3] | Alexandre Roulin[4] | Patrizia Polverino de Laureto[1] | Laura Cendron[3]

[1]Department of Pharmaceutical and Pharmacological Sciences and CRIBI, University of Padova, Padova, Italy

[2]Institute of Microbiology, University Hospital Center and University of Lausanne, Lausanne, Switzerland

[3]Department of Biology, University of Padova, Padova, Italy

[4]Department of Ecology and Evolution, Faculty of Biology and Medicine, University of Lausanne, Lausanne, Switzerland

**Correspondence**
Patrizia Polverino de Laureto, Department of Pharmaceutical and Pharmacological Sciences and CRIBI, University of Padova, 35121 Padova, Italy.
Email: patrizia.polverinodelaureto@unipd.it

Laura Cendron, Department of Biology, University of Padova, 35121 Padova, Italy.
Email: laura.cendron@unipd.it

**Funding information**
Visiting Scientist Programme 2018, University of Padova; University of Padova; Swiss National Science Foundation, Grant/Award Number: 31003A_153467; University of Lausanne; MIUR FFABR, Grant/Award Number: Fondo di Finanziamento per le Attività Base di Ri; MIUR-PNRA, Grant/Award Number: PNRA18_00147; Progetti di Ateneo-University of Padova

Peptides are attractive drugs because of their specificity and minimal off-target effects. Short half-lives are within their major drawbacks, limiting actual use in clinics. The golden standard in therapeutic peptide development implies identification of a minimal core sequence, then modified to increase stability through several strategies, including the introduction of nonnatural amino acids, cyclization, and lipidation. Here, we investigated plasma degradations of hormone sequences all composed of a minimal active core peptide and a C-terminal extension. We first investigated pro-opimelanocortin (POMC) γ2/γ3-MSH hormone behavior and extended our analysis to POMC-derived α-melanocyte stimulating hormone/adrenocorticotropic hormone signaling neuropeptides and neurotensin. We demonstrated that in all the three cases analyzed in this study, few additional residues mimicking the natural sequence alter both peptide stability and the mechanism(s) of degradation of the minimal conserved functional pattern. Our results suggest that the impact of extensions on the bioactivity of a peptide drug has to be carefully evaluated throughout the optimization process.

**KEYWORDS**
drug optimization, in serum stability, melanocyte stimulating hormones, peptide half-life, peptide hormones, pro-opiomelanocortin hormone, proteolysis

## 1 | INTRODUCTION

In the last years, a renewed interest has been raised around peptide-based drugs because they offer both high specificity and selectivity while keeping a low molecular weight that facilitates low cost chemical synthesis.[1–3] A total of 60 peptide-based drugs are currently in the market,[4] and a number of them are in active development.[2] Inspired by the potential applications, peptide-based drugs have been projected as a billion-dollar market.[5]

Despite the numerous advantages, there are a few challenges associated with this class of therapeutics. The inherent weakness of peptide drugs is their poor pharmacokinetic properties, in particular the tendency to be subjected to rapid total proteolysis in vivo that makes the peptide disappear from the bloodstream in a matter of

**Abbreviations:** ACTH, adrenocorticotropic hormone; MSH, melanocyte stimulating hormone; NT, neurotensin.

Luana Palazzi and Antonella Pasquato are contributed equally to this work.

minutes.[6,7] A large number of approaches have been proposed in an attempt to stabilize the peptide backbone to make it resistant to serum degradation. These include, among others, the use of non-natural amino acids, cyclization, lipidation, incorporation of terminal chemical groups, and alteration of the natural sequence.[8–11] The development of a peptide drug with an ideal half-life requires lead chemistry optimization. The very first step is the identification of the bioactive sequence. Next, the exact minimal active core is defined by sequential removal of single amino acids. The minimal unit that keeps full biological activity, normally assessed by in vitro assays, is the unit that undergoes follow-up optimization. This approach arises from the need to minimize side-effects, for example, due to other parts of the molecule where the peptide is embedded in and/or to make the process of drug production effective, "the shorter, the cheaper." On the other hand, while at the early beginning of therapeutic peptides development their sequence never exceeded 10 amino acids, the impressive improvements of peptides selection, synthesis, and modification technologies led to significant length increase of candidates which enter the clinical trials.[12] Modifications are indeed introduced to improve availability and half-lives of each tested peptide drug. In parallel, comprehensive studies cross-correlating stability/activity details are required. That is, activity cannot pay the price for better peptide stability. Efforts to identify the best drug candidate frequently rely on evaluating a large number of compounds. To reduce the number of animal experiments and to time-optimize the study, drugs stability is initially evaluated by in vitro plasma digestion, a widely accepted technique providing reliable predictions of in vivo performance[13].

In this scenario, an interesting peptide system is represented by the pro-opiomelanocortin (POMC) protein complex (Figure 1A,B). Recent studies conducted on peptides derived from bird species and human POMC demonstrated γ3-MSH versus γ2-MSH residual activity after incubation in blood plasma.[14,15] The POMC system consists of α-, β-, and γ-melanocyte stimulating hormones (MSHs) that activate five melanocortin receptors (MC1-5R).[16] MSHs are short peptides (11-18 residues), generated by proteolysis of the common POMC precursor. Each peptide is initially produced as an intermediate extended form, carrying an additional stretch of amino acids at the N- (β-MSH) or C-terminus (γ-MSH and α-MSH). The extended intermediate forms (γ-lipotropin, γ3-MSH, and ACTH) are then subjected to further processing to yield the fully mature hormones (β-MSH, γ2-MSH, and α-MSH) that contain the receptor binding motif "HFRW" (Figure 1A).[17] Maturation of the different peptides occurs intracellularly, throughout the secretory pathway till secretory granules, in a time- and compartment-specific manner, catalyzed by prohormone convertases. Biologically active species are stored in mature granules to be made feasible by secretion upon stimulation.[18] The alignment of γ-MSH sequences reveals striking similarities within the γ2-MSH region. The C-terminal is more variable, in particular an unusual Ser cluster is observed, especially in the barn owl species complex (*Tyto alba*) (Figure 1B).[16] Numerous and diverse biological pathways are regulated by the MC1-5R, including pigmentation, inflammation, energy homeostasis, and steroidogenesis. Given their physiological roles, several MSH-derived ligands with various clinical applications have been developed, ranging from skin inflammation to arthritis and obesity.[19–21] A major problem facing the use of MSHs in clinic is limited plasma half-life. Classical pharmaceutical chemistry structure-activity relationships have been focused on the shorter peptide forms,[22] whereas little is known on the influence of the extra regions on the chemical-physical and biological properties of the hormones per se.

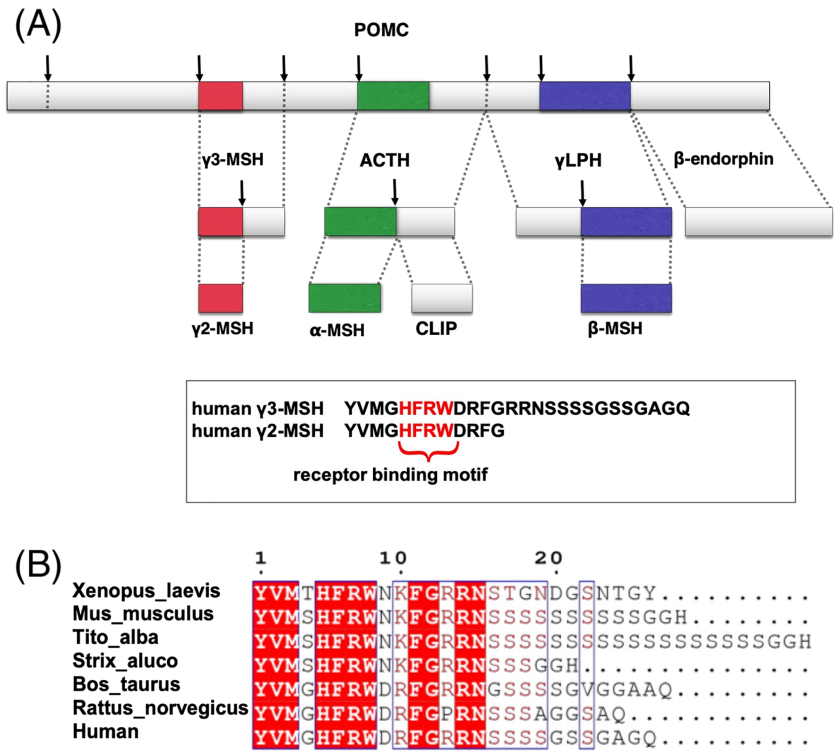


**FIGURE 1** (A) Overview of human pro-opiomelanocortin (POMC) processing pathway in the hypothalamus and the active hormones deriving from such precursor [19]. The primary structure of γ3-MSH and γ2-MSH* is reported, with receptor binding motif highlighted in red. (B) Alignment of human POMC γ3-MSH peptide sequence with representative homologues from other species

Other studies detected a clear difference in stimulatory activity half-life of barn owl and human γ2-MSH and γ3-MSH peptides when exposed to plasma.[16,17] Indeed, in the cell-based assay, the human YVMG**HFRW**DRFG-NH2 (γ2-MSH, in the commercially available amidated form is named γ2-MSH*) loses its ability to stimulate the melanocortin receptor 3 (MC3R) in a few minutes, whereas the analogous YVMG**HFRW**DRFGRRNSSSSGSSGAGQ (γ3-MSH) peptide exhibits a prolonged stimulatory activity under identical conditions. γ2-MSH* and γ3-MSH peptides share identical N-terminus which accommodates the HFRW binding site (Figure 1). As a consequence, the polySer C-terminal extension of γ3-MSH (RRNSSSSGSSGAGQ) has been proposed as a protecting agent causative of the extended biological activity.[17] The issue that arises is if the polySer tail determines this remarkable change in peptide half-lives or they were affected by the different peptides size or conformation. In the present work, we used a combined approach of liquid chromatography and mass spectrometry (MS) to investigate the different behavior in plasma of the human γ2-MSH* and γ3-MSH peptides at the molecular level and to analyze the nature and abundance of the derived species in time course experiments. Our studies not only confirm that the extended peptide does persist intact in human plasma longer when compared with the shorter version but, surprisingly, highlight a completely different degradation mechanism for γ2-MSH* and γ3-MSH, despite they share a large portion of sequence including the recognition site in the N-terminal part. Moreover, to analyze the effect of size or length to explain the different behavior of peptides, we extend our study to other hormone systems, applying the same approach to POMC-derived α-MSH/ACTH and neurotensin signaling peptides. We found that both shorter version of the two peptides (α-MSH and neurotensin 1-13) have limited half-lives when compared with the longer analogues, in agreement with α-MSH/ACTH activity profiles determined by Dores.[17] In both cases, the effect can be attributed to the C-terminal extensions.

## 2 | MATERIALS AND METHODS

### 2.1 | Materials

Peptides were custom-made and purchased from Top-peptide Biotechnology (Shanghai, China), GenScript (Piscataway, NJ, USA), and Bachem (Bubendorf, Switzerland). Human plasma (reconstituted from lyophilized plasma, treated with citrate), enzymes, and enzyme inhibitors were obtained from Sigma-Aldrich (Buchs, Switzerland). All other chemicals were of analytical reagent grade and were obtained from Sigma-Aldrich (Buchs, Switzerland).

### 2.2 | Spectroscopic studies

Peptide concentrations were evaluated from absorption measurements at 280 nm on a Lambda-25 spectrophotometer (Perkin Elmer, Norwalk, CT, USA). The extinction coefficients at 280 nm of γ3-MSH and γ2-MSH* peptides are 6,990 $M^{-1}$ $cm^{-1}$ (2.419 g/l) and 6,990 $M^{-1}$ $cm^{-1}$ (4.619 g/l), of $NT_{1-20}$ and $NT_{1-13}$ are 7,450 $M^{-1}$ $cm^{-1}$ (2.794 g/l) and 2,980 $M^{-1}$ $cm^{-1}$ (1.763), and of ACTH and α-MSH* are 8,480 $M^{-1}$ $cm^{-1}$ (1.867 g/l) and 6,990 $M^{-1}$ $cm^{-1}$ (4.158 g/l) calculated with the method of Gill and von Hippel.[23] Fluorescence emission measurements, after excitation at 280 nm, were conducted with a Perkin Elmer model LS-50B spectrofluorimeter (Norwalk, CT, USA), utilizing a 1-mm × 10-mm path length cuvette. For each measurement, a peptide concentration of 15 μM and a phosphate buffer at pH 7.5, 2.5, or containing 0.2% sodium dodecyl sulfate (SDS) were used. Circular dichroism (CD) spectra were obtained on a J-810 Jasco spectropolarimeter (Tokyo, Japan), equipped with a thermostated cell holder. For the CD measurements, a cell of 1 mm and a peptide concentration of 35 μM were used with a phosphate buffer at pH 7.5 and 2.5 or containing 0.2% SDS.

### 2.3 | Interaction of peptides with plasma

Peptide species were added to human plasma, buffered with triethanolamine (TEA) to pH 7.4, to obtain a final concentration of 40 μM. As a control, milliQ water was added to human plasma. Aliquots from each sample were collected at different times, added to a solution of 6.5% trichloroacetic acid (TCA), and incubated at 4°C for 15 min. To allow the complete precipitation of plasma proteins, the samples were centrifuged at 13,000 rpm for 2 min, at room temperature. The supernatant was collected and analyzed by RP-HPLC (Agilent, mod. 1200, Santa Clara, CA) with a C18 Jupiter column (150 × 4.6 mm, 5 μm, Phenomenex, CA, USA), eluted with a gradient of acetonitrile/0.085% TFA versus water/0.1% TFA from 2% to 38% in 30 min, at a flow rate of 0.6 mL/min. The effluent was monitored by recording the absorbance at 226 nm. The identity of eluted peaks was assessed by MS equipped with an electrospray ionization (ESI) source and a quadrupole (Q)-time-of-flight (TOF) (Micromass, Waters, Manchester, UK) analyzer. The MS analyses were conducted at 1.2 to 1.5 kV capillary voltage and 30 V cone voltage. The pellet was washed with milliQ water and centrifuged at 13,000 rpm for 2 min. MilliQ water was then removed, and 400 μl of 8 M Gnd-HCl, pH 1.5, was added and incubated overnight at 37°C to allow complete pellet dissolution. Centrifugal filters (Amicon Ultra 10000 NMWL, Merck, Darmstadt, DE) were used to fractionate the sample according to their molecular weight. The solubilized pellet was added to filter and centrifuged at 14,000 g for 30 min. The eluate was separated by RP-HPLC, and the chromatographic peaks were analyzed by MS. Phosphoramidon inhibition experiment was conducted adding 10 μM inhibitor to the plasma before the incubation with the peptides.[24]

### 2.4 | Susceptibility to proteolysis

The proteolysis reactions with endoproteinase AspN (EC 3.4.24.33), proteinase K (pK) from *Tritirachium album* (EC 3.4.21.64), and endoproteinase GluC (*Staphylococcus aureus* Protease V8) (EC 3.4.21.19)

were conducted at specific pH and temperature (pH 7.5 and 37°C for AspN; pH 7.5 and 22°C for pK; pH 5.5 and 37°C for GluC) by using a molar enzyme:substrate (E:S) of 1:500 or 1:1,000. Aliquots from the proteolysis mixtures were withdrawn at indicated time of incubation, and the reactions were quenched with an equal volume of aqueous TFA at 0.2%. The different time points were collected and analyzed by RP-HPLC (Agilent, mod. 1,200, Santa Clara, CA) with a C18 Jupiter column (150 × 4.6 mm, 5 μm, Phenomenex, CA, USA), eluted with the following acetonitrile/0.085% TFA-water/0.1% TFA gradient: 2% to 40%, 30 min. The identity of the peptide fragments separated by RP-HPLC was assessed by ESI-MS with a Q-Tof micro mass analyzer (Micromass, Manchester, UK).

### 2.5 | Aggregation experiment

To verify intrinsic tendency to aggregate, peptides were dissolved in phosphate buffer saline buffer, pH 7.5, or in the same buffer containing 6 M guanidine hydrochloride (Gnd-HCl). Aliquots from the solution were withdrawn and analyzed by RP-HPLC. The analyses were conducted by using a C18 Jupiter column (150 × 4.6 mm, 5 μm, Phenomenex, CA, USA), eluted with the following acetonitrile/0.085% TFA-water/0.1% TFA gradient: 2% to 40%, 30 min. The effluent was monitored by recording the absorbance at 226 nm.

## 3 | RESULTS AND DISCUSSION

### 3.1 | Human γ2-MSH*peptide is degraded faster than γ3-MSH in human plasma

*Tyto alba* and human to -MSH peptides retained longer biological activity in plasma when including C-terminal natural extensions.[14,15] Here, we opted for the (bio)-chemical analysis of synthetic human analogues γ2-MSH* (YVMGHFRWDRFG-$NH_2$) and γ3-MSH (YVMGHFRWDRFGRRNSSSSGSSGAGQ) (Table 1, Figure 1B). Since biological activity is a downstream readout to the actual concentration of the MSHs, we first investigated whether this reading directly correlates with a different decay of the two peptides in plasma. Briefly, γ2-MSH* and γ3-MSH were incubated at 37°C with human plasma buffered at pH 7.4 and samples collected at several time points over few hours. Aliquots were subjected to precipitation by TCA to eliminate plasma components. The pellets were resuspended in acidic and denaturing conditions and filtered prior to chromatographic separation, while the supernatants were directly analyzed by RP-HPLC. The peptide components were identified by electrospray (ESI)–quadrupole Q-Tof MS.

As shown in Figure 2B,C, γ2-MSH* (retention time [RT] 43.7 min) decreased over time more rapidly than γ3-MSH (RT 41.2 min). The shorter but not the longer peptide underwent a massive decay in the very first minutes of incubation (∼80% vs. ∼25% at 15 min, Figure 2C). Analysis of the pellet showed that both peptides precipitate with plasma, accumulating in the insoluble fraction. Moreover, a fraction of deamidated (+1 Da) γ2-MSH* was also found in the pellet (Figure 3). To exclude that the chemical treatment with TCA could act as major precipitating agent, recovery yields of peptides from plasma were calculated (Table 2). The recovery yield was obtained evaluating the area of the HPLC peptide peaks after their incubation with plasma, pretreated by pan-protease inhibitors, and it was estimated to be approximately 29% and 12%, for γ3-MSH and γ2-MSH*, respectively (Table 2). Such results could be explained by the interaction of both peptides with plasma proteins. Indeed, when TCA was added to the pure peptide solution, γ3-MSH and γ2-MSH* recovery in the supernatant was at least three times higher. In order to verify if peptides underwent self-aggregation under our experimental conditions (pH 7.4), γ3-MSH and γ2-MSH* samples were incubated either in PBS pH 7.4 or in the same buffer supplemented with 6 M Guanidine-HCl. Aliquots of the samples were collected at specific times and analyzed by RP-HPLC (Figure S1). The RT, intensity, and shape of RP-HPLC peaks from both samples incubated at pH 7.4 and under denaturing conditions overlapped and did not change over time (5 h), showing a scarce tendency of the peptides to aggregate within the considered experimental interval of time.

**TABLE 1** Sequence and chemical characterization of the peptide species used in this work

| Name | Sequence | MW (Da) |
|---|---|---|
| γ2-MSH* | YVMGHFRWDRFG | 1,568.75 |
| γ3-MSH | YVMGHFRWDRFGRRNSSSSGSSGAGQ | 2,888.33 |
| $NT_{1-13}$ | QLYENKPRRPYIL | 1,688.94 |
| $NT_{1-20}$ | QLYENKPRRPYILKRDSYYY | 2,664.38 |
| α-MSH | SYSMEHFRWGKPVG | 1,679.79 |
| $ACTH_{1-39}$ | SYSMEHFRWGKPVGKKRRPVK VYPNGAEDESAEAFPLEF | 4,541.13 |

*Note.* The masses are calculated referring to the amino acid sequence and using the residue monoisotopic weight. For ACTH, the averaged molecular weight is reported.

Abbreviations: ACTH, adrenocorticotropic hormone; MSH, melanocyte stimulating hormone; NT, neurotensin.

*C-terminal amino acid is in the amidated form.

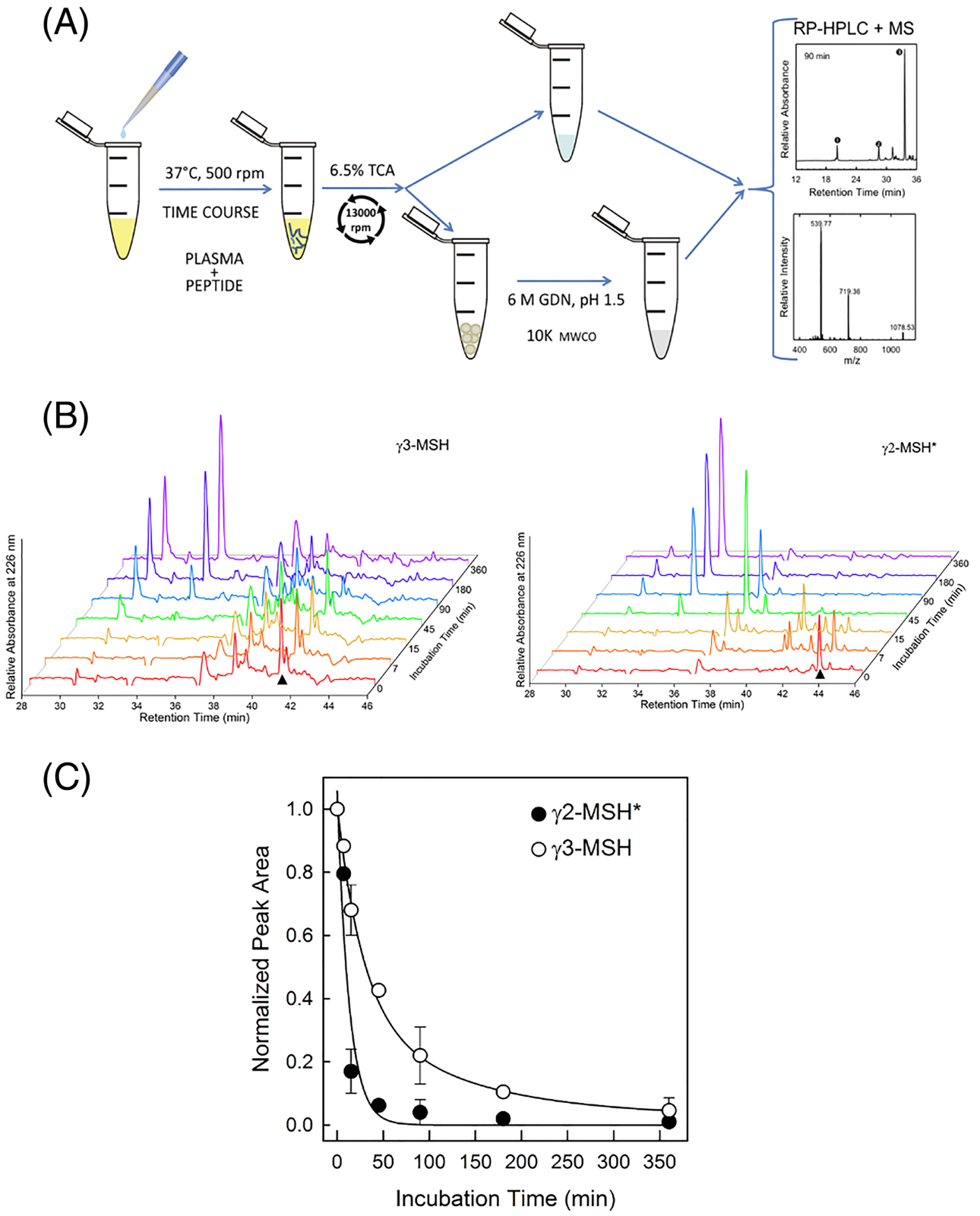


**FIGURE 2** (A) Scheme of the experimental set up: the kinetic analysis was performed by RP-HPLC of samples collected from the peptide-plasma mixture at defined time intervals. Aliquots were subjected to precipitation by trichloroacetic acid (TCA) to eliminate plasma components. Resulting supernatants were analyzed by RP-HPLC and peptides were identified by MS. (B) RP-HPLC profiles of γ3-MSH and γ2-MSH* samples analyzed at defined incubation time intervals; plasma contribution (blank run) has been subtracted from all the HPLC profiles. The peaks highlighted by a black triangle correspond to the full-length peptide species. (C) Trend of γ3-MSH (empty circles) and γ2-MSH* (black circles) peptides half-life. The curves were obtained plotting the area of the peaks relative to the full-length peptides estimated by RP-HPLC versus incubation time. The reported values have been calculated from triplicates

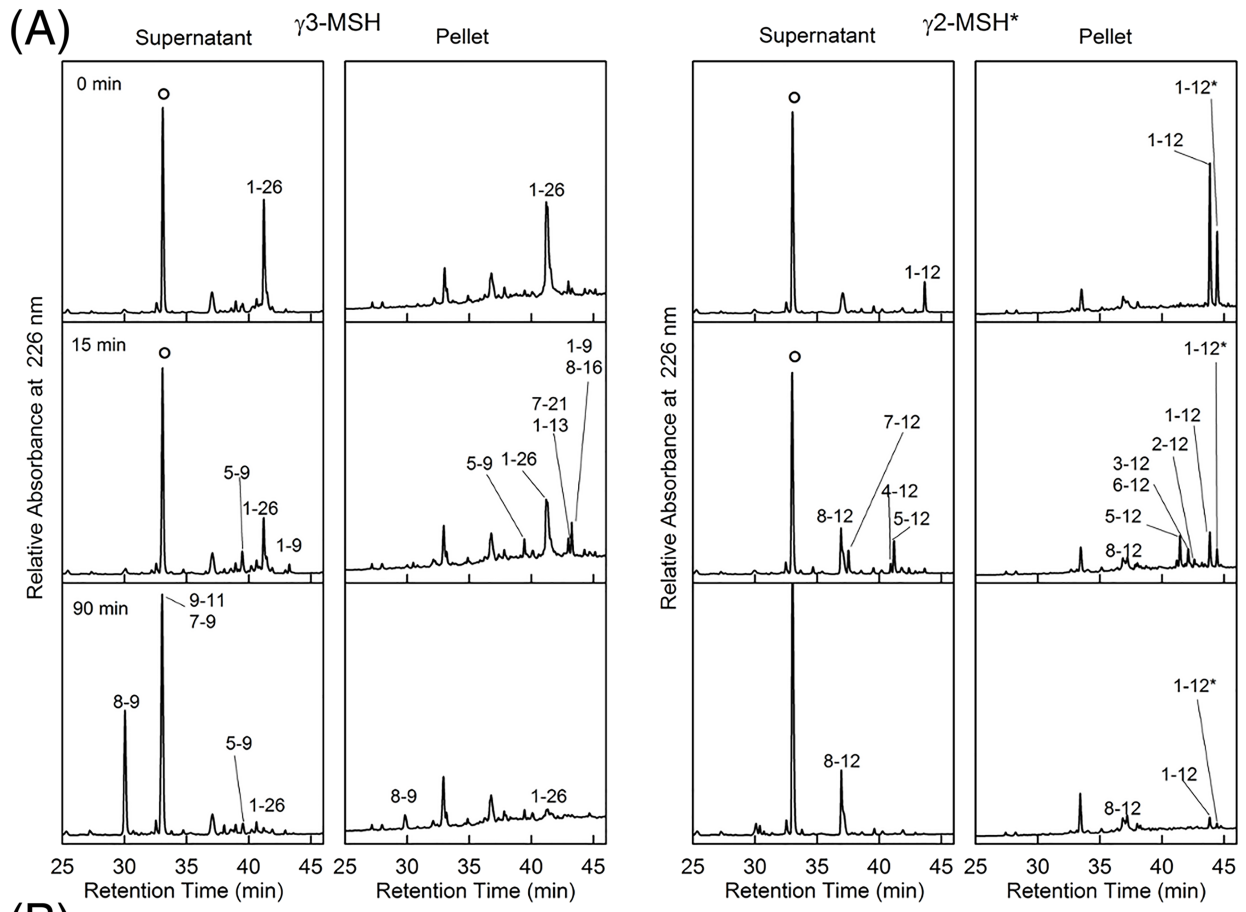


(B)

| γ3-MSH peptide species | | 0 | 15 | 90 |
|---|---|---|---|---|
| 1-26 | YVMGHFRWDRFGRRNSSSSGSSGAGQ | ++++ | +++ | + |
| 1-13 | YVMGHFRWDRFGR | - | - | ++++ |
| 1-9 | YVMGHFRWD | - | ++++ | - |
| 5-9 | HFRWD | - | ++++ | + |
| 5-6 | HF | - | - | ++++ |
| 7-21 | RWDRFGRRNSSSSGS | - | ++++ | +++ |
| 7-20 | RWDRFGRRNSSSSG | - | - | ++++ |
| 7-19 | RWDRFGRRNSSSS | - | - | ++++ |
| 7-9 | RWD | - | - | ++++ |
| 8-24 | WDRFGRRNSSSSGSSGA | - | - | ++++ |
| 8-9 | WD | - | - | ++++ |
| 9-11 | DRF | - | - | ++++ |

| γ2-MSH* peptide species | | 0 | 15 | 90 |
|---|---|---|---|---|
| 1-12 | YVMGHFRWDRFG | ++++ | + | - |
| 2-12 | VMGHFRWDRFG | - | ++++ | - |
| 3-12 | MGHFRWDRFG | - | ++++ | - |
| 4-12 | GHFRWDRFG | - | ++++ | - |
| 5-12 | HFRWDRFG | - | ++++ | - |
| 5-6 | HF | - | - | ++++ |
| 6-12 | FRWDRFG▲ | - | ++++ | - |
| 7-12 | RWDRFG | - | ++++ | - |
| 8-12 | WDRFG | - | ++ | ++++ |
| 9-12 | DRFG | - | - | ++++ |
| 10-12 | RFG | - | +++ | ++++ |

**FIGURE 3** (A) RP-HPLC time course analysis of γ3-MSH and γ2-MSH* peptides incubated with human plasma. The fractions corresponding to 0, 15, and 90 min, treated as reported in Figure 2A, and separated in pellet and supernatant are reported. RP-HPLC analysis of both solubilized pellet and supernatant samples are shown side by side in the picture. The empty circle indicates peaks deriving from plasma contribution. For clarity, only the most significant retention time intervals have been selected and reported. (B) Scheme of fragmentation yield of γ3-MSH (left) and γ2-MSH*(right) upon incubation with plasma. The first column refers to the identified peptide, the second to its sequence, and the third to the relative distribution of peptide species after different incubation times in plasma (0, 15, and 90 min). The groups of peptides starting (red) or ending (blue) with the same residue are highlighted. The peptide yield has been normalized for each peptide species to the highest amount of this species at any of the three time points using a scale from 0 (–) to 1 (++++) with the following intermediate points: 0.25 (+), 0.5 (++), and 0.75 (+++). The symbol black triangle indicates species found in the pellet

**TABLE 2** Yield (percent) of recovery of γ-MSH peptides after plasma (P) exposure and treatment with trichloroacetic acid (P + TCA) or with TCA only (TCA)

| Peptides recovery | | |
|---|---|---|
| | P + TCA (%) | TCA (%) |
| γ3-MSH | 29.4 ± 6 | 93.2 ± 5 |
| γ2-MSH* | 11.7 ± 4 | 74.4 ± 8 |

*Note.* Plasma contained a mixture of protease inhibitors. The calibration curve was obtained from the areas of the peptides alone.
Abbreviations: MSH, melanocyte stimulating hormone; TCA, trichloroacetic acid.

## 3.2 | The mechanism of degradation of γ2-MSH* implies N-terminal proteolysis and splitting at aromatic residues level

After confirming the shorter half-life of γ2-MSH*, in order to clarify the molecular mechanism, we focused our attention on the numerous RP-HPLC peaks generated by plasma incubation (Figures 2 and 3). Each fragment was identified by MS (Table 3) and, if necessary, by MS/MS (not shown). We found that N-terminal truncated fragments followed the rapid disappearance of full length γ2-MSH*. Removal of each amino acid was sequential, suggesting the action of plasma amino-peptidase(s) (Figure 3, Table 3). The mechanism implies that each newly generated species serves as substrate for the following N-terminal residue cleavage (Figure 3B, right). All truncations, from 2-12 to 10-12 fragments, were recovered from the supernatant, with the exception of the 6-12 fragment, detectable only in the pellet. The relative amount of the species was calculated by evaluating the area of the RP-HPLC peaks obtained at 226 nm at each time point. Over time, species truncated up to residue Arg7 accumulated and later (90 min) disappeared upon incubation. An opposite trend was observed for the species truncated after Arg7 (Figure 3). Endo-protease activity was also present, although to a less significant degree, to give $_5$HF, $_7$RW$_8$, and $_9$DRF$_{11}$ fragments (Table 3). All these peptides share an aromatic residue at the C-terminus, opening to the possibility that the protease responsible for the cleavage privileges F/W/Y at P1. A likely candidate is neprilysin (NEP), a Zn metallo-protease anchored to the plasma membrane and eventually shed into the blood stream.[25,26] The enzyme has a preference toward peptides over proteins and is well known as degrading agent of a variety of physiologically relevant hormones such as enkephalins, tachykinins,[27] and amyloid peptides.[28] Blocking NEP activity is clinically relevant. For example, Sacubitrilat is a Food and Drug Administration (FDA)–approved inhibitor of NEP used to treat heart failure via blocking vasodilatation.[29] Given the role of γ-MSHs in natriuresis[30] and therefore vasodilatation, and the presence of a "NEP cleavage signature" upon plasma incubation, we investigated whether this endo-protease is involved in γ2-MSH* degradation. To this aim, we used the commercially available phosphoramidon inhibitor.[24] Overall, there is a slow-down formation of specific fragments. Sequences carrying aromatic residues at the C-terminus were delayed or, as in the case of 5-6 and 9-12 fragments,

**TABLE 3** Chemical characterization of γ-MSH peptide species upon exposure to plasma collected from the supernatant or contained in the pellet isolated by RP-HPLC (Figure 3)

| | RT[a] (min) | Molecular Mass (Da) | | Peptide species |
|---|---|---|---|---|
| | | Found[b] | Calculated[c] | |
| γ3-MSH | 30.1 | 319.12±0.01 | 319.12 | 8-9 |
| | 30.8 | 1812.81 ±0.03 | 1812.83 | 8-24 |
| | | 1609.78 ±0.02 | 1609.78 | 7-19 |
| | | 1666.85 ±0.02 | 1666.80 | 7-20 |
| | 31.0 | 302.11±0.01 | 302.14 | 5-6 |
| | 33.1 | 475.31±0.01 | 475.22 | 7-9 |
| | | 436.21±0.01 | 436.21 | 9-11 |
| | 34.7 | 360.31±0.01 | 360.19 | 7-8 |
| | 39.5 | 759.41±0.01 | 759.35 | 5-9 |
| | 41.2 | 2889.01 ±0.02 | 2888.33 | 1-26 |
| | 43.0 | 1726.04 ±0.02 | 1725.83 | 1-13 |
| | | 1753.77 ±0.04 | 1753.84 | 7-21 |
| | 43.3 | 1209.80 ±0.02 | 1209.54 | 1-9 |
| | | 1192.33 ±0.01 | 1192.59 | 8-16 |
| γ2-MSH* | 30.2 | 493.34 ±0.01[d] | 492.24 | 9-12 |
| | 30.9 | 302.15±0.01 | 302.14 | 5-6 |
| | 33.1 | 436.27±0.01 | 436.21 | 9-11 |
| | 33.7 | 378.21 ±0.02[d] | 377.21 | 10-12 |
| | 34.8 | 360.33±0.01 | 360.19 | 7-8 |
| | 36.9 | 678.46±0.02 | 678.32 | 8-12 |
| | 37.5 | 834.45±0.01 | 834.42 | 7-12 |
| | 40.9 | 1176.41 ±0.01[d] | 1175.57 | 4-12 |
| | 41.2 | 1119.64 ±0.01[d] | 1118.55 | 5-12 |
| | 41.9 | 1307.27 ±0.01[d] | 1306.61 | 3-12 |
| | | 981.30±0.01 | 981.49 | 6-12 |
| | 42.5 | 1406.40 ±0.01[d] | 1405.68 | 2-12 |
| | 43.7 | 1568.91 ±0.01 | 1568.75 | 1-12 |

Abbreviations: MSH, melanocyte stimulating hormone; RT, retention time.
[a]Peptides are listed in order of RT in RP-HPLC.
[b]Experimental molecular masses determined by ESI-QTOF-MS.
[c]Theoretical masses calculated on the base of the amino acid sequence.
[d]These masses refer to free acid form of the peptide.

absent (Figure S2), suggesting γ2-MSH* as a novel NEP substrate. Eventually, the inhibition did not block the disruption of the peptide by plasma proteases. The results were in line with expectations since γ2-MSH* degradation most likely involves amino peptidases which act upstream and/or independently from the formation of NEP fragments. The physiological role of NEP/γ-MSH interaction, here proposed, must be further investigated to be validated.

The rapid destruction of the HFRW motif no more conserved in any of the detected species after 15 min of incubation justifies the likewise rapid decay of the reported biological activity in plasma[15].

### 3.3 | γ3-MSH degradation requires endo-proteolysis to generate WD dipeptide as main cleavage product

γ3-MSH peptide digestion was performed and analyzed in parallel to γ2-MSH*, using identical conditions and protocols. Overall, we faced a strikingly different scenario: (a) the supernatant was not fully representative of most of the degradation products; (b) by RP-HPLC, some fragments coeluted with plasma molecules (Figure A, Table 3). The former aspect made the overall analysis challenging because the expected sequences fully disappeared from the soluble and insoluble fractions. By comparison, all γ2-MSH* products but one were represented in the supernatant of γ3-MSH. The RP-HPLC profiles, supported by MS analysis, uncovered an unexpected mechanism of digestion of γ3-MSH in comparison with γ2-MSH* peptide. First of all, γ3-MSH showed a longer half-life than γ2-MSH*. Furthermore, despite the peptides exhibited an identical N-terminal sequence, they underwent a completely different cleavage pattern. In fact, upon prolonged incubation of γ3-MSH with plasma, the main fragments were $_{7}$RWD$_{9}$ and $_{8}$WD$_{9}$ that were not found in γ2-MSH* mixture. In total, 13 different peptide fragments were identified (Table 3). Two out of 13 started from Trp residue at position 8, four ended at Asp residue at position 9, and four fragments started from Arg residue at position 7 (Figure 3B, left). Of note, the first cleavage sites (15 min) were located at the level of Arg7-Trp8 and Asp9-Arg10 peptide bonds. After prolonged incubation time (90 min), two different proteolysis patterns were visible. In one case, fragments ending with the residue Asp9 or starting with Arg7 underwent further proteolysis giving rise to the species $_{7}$RWD$_{9}$ and $_{8}$WD$_{9}$, as the main cleavage products, indicating that these fragments were produced only after that their terminal residue was available. In the other case, peptides still containing the C-terminal tail became progressively more susceptible to the proteolysis losing one by one the amino acid from the C-terminal. Overall, we observed an unexpected mechanism of degradation for γ3-MSH. The uniqueness of our discovery relies on the observation that two peptides sharing identical N-termini undergo completely different pathways of cleavage when exposed to the same degradative conditions. The very soft spot at the N-terminus of γ2-MSH* becomes somehow very resistant when few amino acids are added at the C-terminus (γ3-MSH). Notably, the tail is located more than 10 residues far away from the cleavage site. In turn, new bonds are made more susceptible to cleavage, taking the degradative profile upside-down.

### 3.4 | γ2-MSH* and γ3-MSH are intrinsically recognized by proteases in a different manner

It appears clear that the two γ2-MSH* and γ3-MSH peptides are differently digested in plasma and that γ3-MSH shows a striking resistance when compared with the shorter homologue. These experiments are challenging since several factors can contribute to the final effect; so to verify the intrinsic peptide susceptibility to protease attack, we used a very simplified system where the only variables were the enzymes and their substrates. Asp-N, endoproteinase GluC, and proteinase K (pK) were the three enzymes used in this set of experiments.[31] AspN is a very well-characterized endoproteinase used to produce protein digests for peptide mapping and protein sequence.[32] AspN cleaves primarily before the Asp residue which is present in both γ2-MSH* and γ3-MSH within the shared sequence. Peptides were incubated with AspN in phosphate buffer and samples collected over 300 min to monitor cleavability and kinetics of processing. MS analysis confirmed cleavage occurred only at Asp9, according to expectations (Figure S3, Table S1). Both peptides were susceptible to AspN activity and fully digested. However, γ2-MSH* required more than 1 h to disappear, whereas γ3-MSH was processed very quickly, with an estimated greater than 50% degradation within the very first 5 min of incubation with the protease (Figure 4A; Figure S3). Thus, the Ser-rich tail in γ3-MSH was not only incapable of protection, but it seemed to favor the process of peptide processing. This finding is in line with the observation that cleavage around $_{8}$WD$_{9}$ was very favorable only for the γ3-MSH peptide. Indeed, in plasma, γ3-MSH is not degraded from the N-terminal, in contrast with γ2-MSH, which is primarily substrate for the plasma aminoproteases.

We next digested both peptides with GluC, an endoproteinase which recognizes and cleaves after acidic residues.[33] GluC prefers Glu over Asp, and specificity can be switched using the appropriate buffer. Thus, γ2-MSH* and γ3-MSH were incubated in phosphate buffer pH 5.5 to favor cleavage after Asp residue and the digestion was monitored as reported above. Interestingly, none of the substrates were cleaved by GluC (Figure S3). Further attempts were made changing conditions and prolonging the time of incubation up to 24 h, but no cleavage products were observed (Figure S3). On-target enzymatic activity of GluC was verified by human albumin, digested in parallel to peptides. Despite the presence of acidic residues on both sequences, GluC exposure did not affect peptides stability, and such behavior is in line with a not strictly predictable degradation profile, simply based on sequence features. Finally, the two peptides were incubated with pK, an enzyme with preference toward aliphatic/aromatic residues (Figure S3). Proteinase K is commonly used for its broad specificity; indeed, it usually catalyzes the hydrolysis of peptides formed by the most diverse amino acid residues within a disordered region of a protein.[34] We found that γ2-MSH* and γ3-MSH were cleaved at Arg6 with similar kinetics (Figure 4B). Indeed, the percentage of cleavage at 5 min

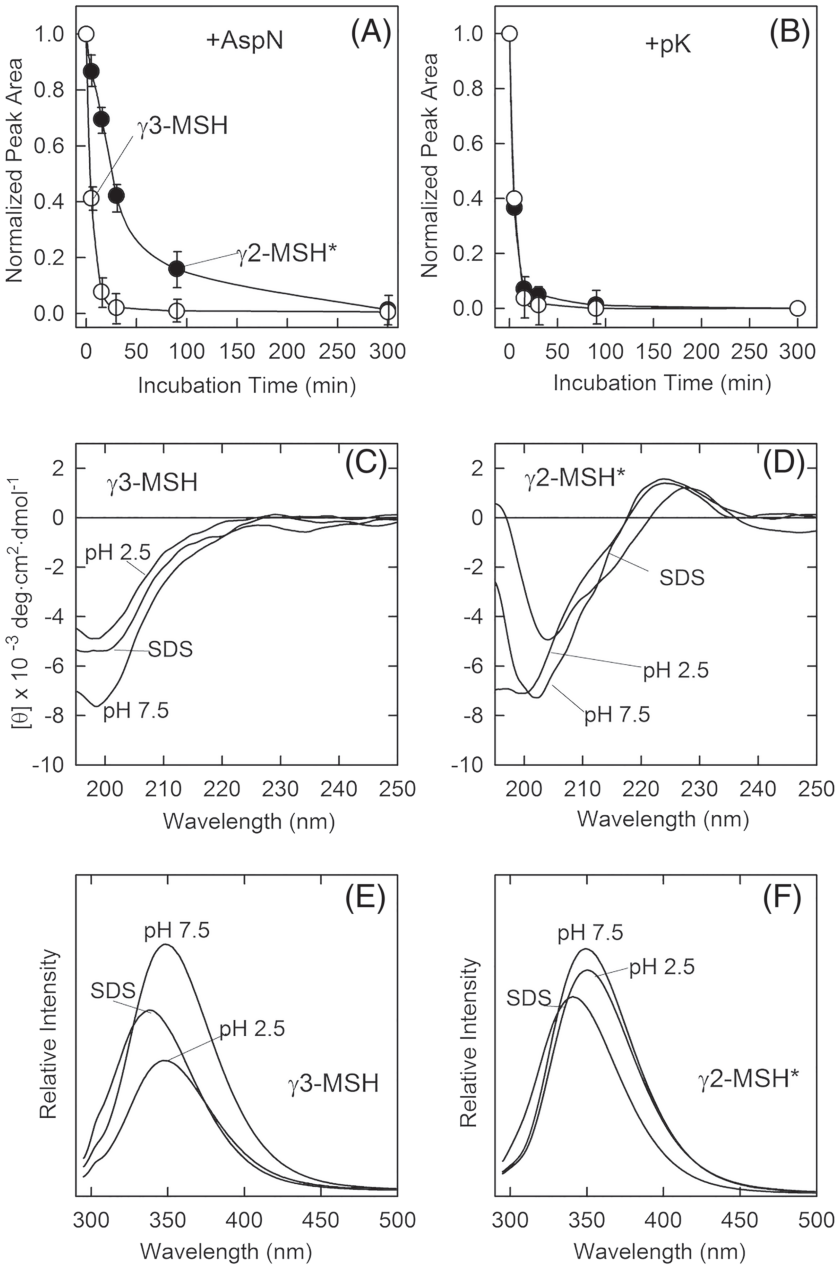


**FIGURE 4** Structural characterization of γ-MSH peptides. (A and B) Proteolysis susceptibility analysis. The profiles of γ3-MSH (empty circle) and γ2-MSH* (black circle) peptides consumption upon in vitro incubation with proteases, (A) AspN and (B) pK, are represented. The area of the peaks, estimated by RP-HPLC , is plotted against incubation time. Conformational characterization of γ3-MSH and γ2-MSH* peptides by circular dichroism in the (C and D) far UV and (E and F) fluorescence spectroscopy. Molar ellipticity has been recorded between 195 and 250 nm; tryptophan fluorescence has been excited at 280 nm, and emission signal was registered between 290 and 500 nm. Peptides structural changes has been followed at pH 7.5, 2.5 and upon 0.2% SDS detergent treatment with both techniques

is approximately 62% for γ2-MSH* and approximately 60% for γ3-MSH (Figure S3), resulting in comparable [1-6]/[7-12] and [1-6]/[7-26] fragment ratios, respectively. Longer incubations induced further fragmentations with appearance of multiple shorter sequences (Figure S3, Table S1). $_{1}$YVMGHF$_{6}$ was the most unstable and got attacked after Met3 to eventually disappear as for γ2-MSH*. In contrast, $_{7}$RWDRFG$_{12}$ showed an unexpected persistence in γ2-MSH*. The more extended $_{7}$RWDRFGRRNSSSSGSSGAGQ$_{26}$ γ3-MSH fragment was resistant and underwent cleavage limited to the Asn residue.

Overall, we showed that γ2-MSH* per se is not more cleavable than γ3-MSH. On the contrary, the longer peptide is more (AspN) or equally (GluC and pK) susceptible to degradation when compared with the shorter analogue. Our studies infer that the presence of the polySer tail enhances γ3-MSH propensity to be processed in close proximity to the WD motif. In this context, we should mention that Trp containing bioactive dipeptides have been the subject of recent studies. In particular, both WE (Trp-Glu) and WR (Trp-Arg) have been demonstrated to bind and stimulate the activity of peroxisome proliferator-activated receptor (PPAR) α, inducing a cascade of events which cause reduced lipid accumulation in hepatocytes.[35,36] Such findings open the hypothesis of a biological role, other than MCR3 stimuli, for γ3-MSH hormone, which should be investigated in the future.

In conclusion, the sequence extension of γ3-MSH is capable of modulating the half-life of the peptide and, most importantly, its mechanism of degradation. Local conformation seems not to contribute to this phenomenon for γ-MSH peptides. The outcomes depend on the complex interaction of the extended substrate with specific proteases.

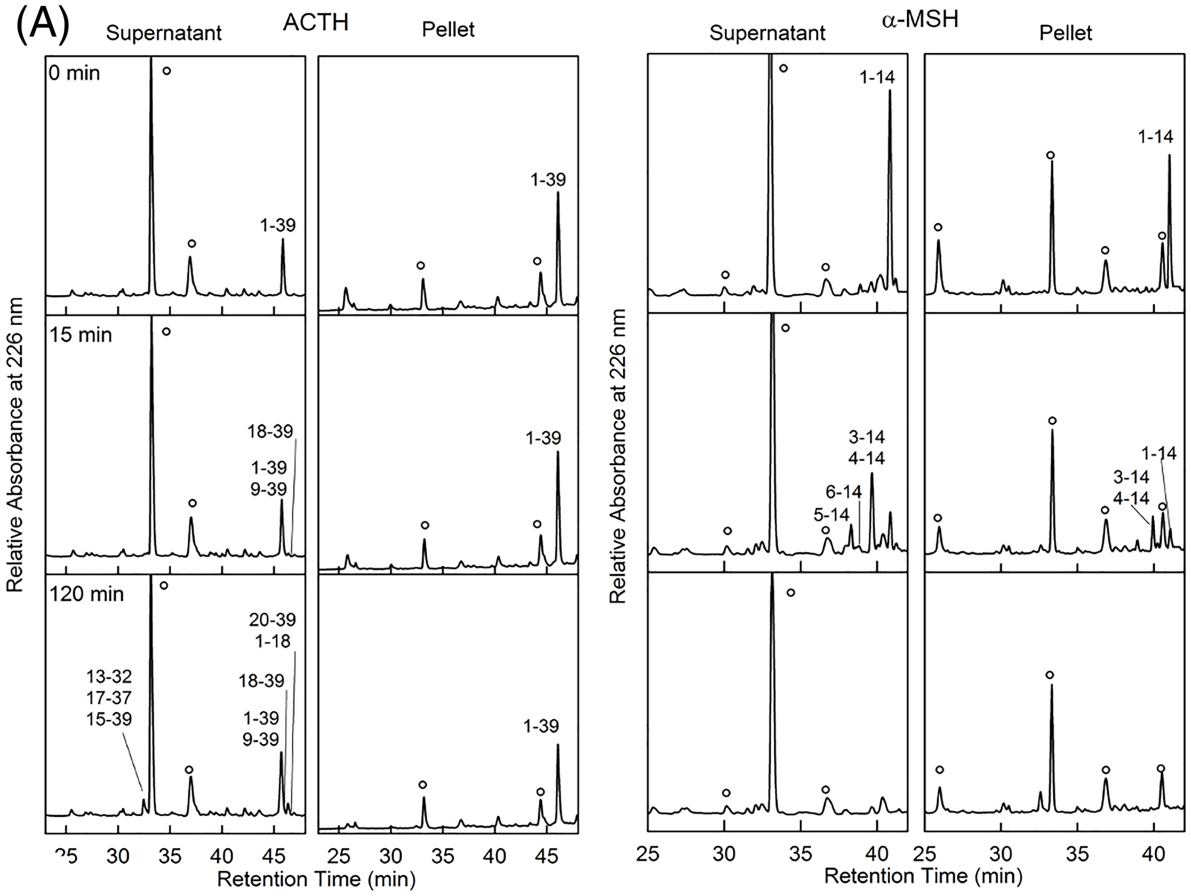


| ACTH peptide species | | 0 | 15 | 480 |
|---|---|---|---|---|
| 1-39 | SYSMEHFRWGKPVGKKRRPVKVYPNGAEDESAEAFPLEF | ++ ++ | ++ ++ | + |
| 1-37 | SYSMEHFRWGKPVGKKRRPVKVYPNGAEDESAEAFPL | - | - | ++ ++ |
| 1-18 | SYSMEHFRWGKPVGKKRR | - | - | ++ ++ |
| 1-15 | SYSMEHFRWGKPVGK | - | - | ++ ++ |
| 2-15 | YSMEHFRWGKPVGK | - | - | ++ ++ |
| 3-15 | SMEHFRWGKPVGK | - | - | ++ ++ |
| 3-14 | SMEHFRWGKPVG | - | - | ++ ++ |
| 9-39 | WGKPVGKKRRPVKVYPNGAEDESAEAFPLEF | - | + | ++ ++ |
| 9-37 | WGKPVGKKRRPVKVYPNGAEDESAEAFPL | - | - | ++ ++ |
| 14-37 | GKKRRPVKVYPNGAEDESAEAFPL | - | - | ++ ++ |
| 15-39 | KKRRPVKVYPNGAEDESAEAFPLEF | - | - | ++ ++ |
| 17-37 | RRPVKVYPNGAEDESAEAFPL | - | - | ++ ++ |
| 18-39 | RPVKVYPNGAEDESAEAFPLEF | - | + | ++ ++ |
| 18-38 | RPVKVYPNGAEDESAEAFPLE | - | - | ++ ++ |
| 18-37 | RPVKVYPNGAEDESAEAFPL | - | - | ++ ++ |
| 20-39 | VKVYPNGAEDESAEAFPLEF | - | - | ++ ++ |
| 22-39 | VYPNGAEDESAEAFPLEF | - | - | ++ ++ |
| 23-31 | YPNGAEDES | - | - | ++ ++ |

| α-MSH peptide species | | 0 | 15 | 480 |
|---|---|---|---|---|
| 1-14 | SYSMEHFRWGKPVG | ++ ++ | + | - |
| 3-14 | SMEHFRWGKPVG | - | ++ ++ | - |
| 4-14 | MEHFRWGKPVG | - | ++ ++ | - |
| 5-14 | EHFRWGKPVG | - | ++ ++ | - |
| 6-14 | HFRWGKPVG | - | ++ ++ | - |

**FIGURE 5** The case of α-melanotropin/adrenocorticotropin, α-MSH/ACTH peptides. (A) RP-HPLC kinetic analysis of ACTH and α-MSH peptides incubated with human plasma. RP-HPLC chromatograms of fractions collected at different times (0, 15, and 120 min), treated as described for γ-MSH peptides. The empty circle indicates peaks deriving from plasma. Most significant retention time intervals have been reported. (B) Scheme of fragmentation of ACTH/α-MSH peptides incubated with human plasma, as deduced from RP-HPLC and MS analysis. The first column refers to the peptide, the second to the sequence of the peptide, and the third to time of incubation with plasma (0, 15, and 480 min). Peptides starting (red) or ending (blue) with the same residue are shown. The peptide yield has been normalized by the scale described in Figure3

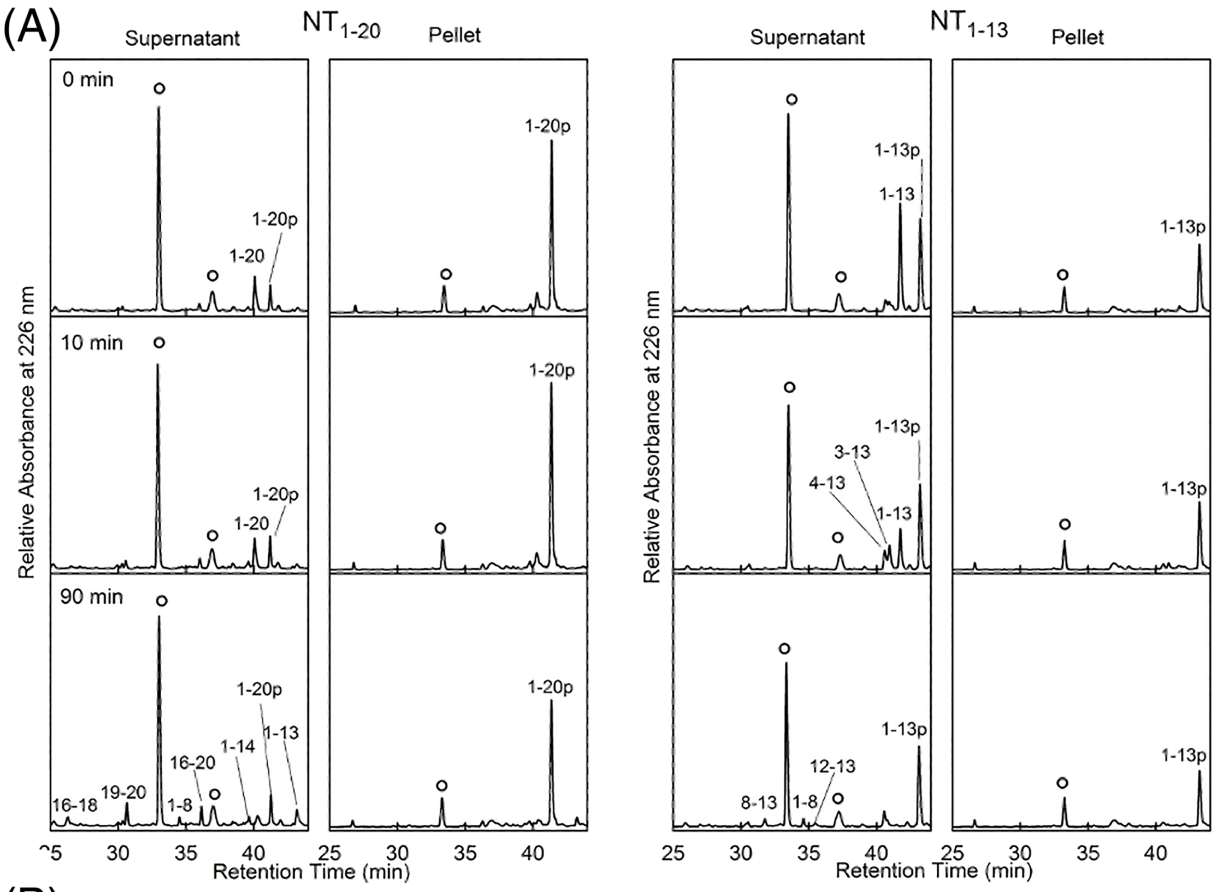


(B)

| $NT_{1-20}$ peptide species | | 0 | 10 | 90 |
|---|---|---|---|---|
| 1-20 | QLYENKPRRPYILKRDSYYY | ++ ++ | ++ + | - |
| 1-20p | QLYENKPRRPYILKRDSYYY | ++ + | ++ ++ | ++ ++ |
| 1-20p | QLYENKPRRPYILKRDSYYY▲ | ++ ++ | ++ ++ | ++ + |
| 1-14p | QLYENKPRRPYILK | - | ++ + | ++ ++ |
| 1-13p | QLYENKPRRPYIL | - | - | ++ ++ |
| 1-8p | QLYENKPR | - | - | ++ ++ |
| 16-20 | DSYYY | - | - | ++ ++ |
| 16-18 | DSY | - | - | ++ ++ |
| 19-20 | YY | - | + | ++ ++ |

| $NT_{1-13}$ peptide species | | 0 | 10 | 90 |
|---|---|---|---|---|
| 1-13 | QLYENKPRRPYIL | ++ ++ | ++ | - |
| 1-13p | QLYENKPRRPYIL | ++ + | ++ ++ | ++ ++ |
| 1-13p | QLYENKPRRPYIL▲ | ++ ++ | ++ ++ | ++ + |
| 1-8p | QLYENKPR | - | - | ++ ++ |
| 3-13 | YENKPRRPYIL | - | ++ ++ | + |
| 4-13 | ENKPRRPYIL | - | ++ ++ | ++ + |
| 8-13 | RRPYIL | - | + | ++ ++ |
| 12-13 | IL | - | + | ++ ++ |

**FIGURE 6** The case of Neurotensin, $NT_{1-13}$/$NT_{1-20}$ peptides. (A) RP-HPLC kinetic analysis of $NT_{1-13}$/$NT_{1-20}$ peptides incubated with human plasma. RP-HPLC chromatograms of fractions collected at different times (0, 10, and 90 min), treated as described for γ-MSH peptides. The empty circle indicates peaks deriving from plasma. (B) Most significant retention time intervals have been reported. Scheme of fragmentation of $NT_{1-13}$/$NT_{1-20}$ peptides incubated with human plasma, as deduced from RP-HPLC and mass spectrometry (MS) analysis. The analysis was conducted as described in Figures 3 and 5. The suffix p refers to the pyroglutamic form of the peptide, and the triangle indicates the peptide isolated and identified in the pellet

### 3.5 | γ2-MSH* and γ3-MSH are disordered in solution

It is commonly accepted that the peptide structure around the cleavage site can alter the kinetics of proteolysis.[37,38] We next investigated whether the C-terminal tail was determinant for inducing or disrupting specific conformations, for example, β-turns, important for peptide processing.[38,39] To this aim, γ2-MSH* and γ3-MSH were analyzed by far UV-CD spectroscopy in several means (pH 7.5, pH 2.5, 0.2% SDS). All the tested conditions revealed the absence of any structure and clear propensity to adopt random conformation for both peptides (Figure 4C,D). Studies were further extended to intrinsic fluorescence analysis to better understand the accessibility of $Trp_8$. This tryptophan represents the soft spot within the γ3-MSH peptide.[40] The emission maximum at 350 nm suggested that the aromatic residue is exposed to solvent and characterized by a very similar exposure in both γ2-MSH* and γ3-MSH at pH 7.5 and 2.5. In the presence of 0.2% SDS, fluorescence profiles persisted, except a slight shift toward shorter wavelength, meaning a randomness state of the polypeptide chains (Figure 4E,F).

Taken together, we state the inability of the polySer tail to induce preference toward any specific conformation. The shorter hormone is found in a random conformation that persists also in the longer version. Thus, it is conceivable that the tail may rather influence the interaction among peptide and plasma proteins, including plasma proteases.

### 3.6 | The protection mechanism can be translated to other peptide systems

Human γ3-MSH survives in plasma longer than γ2-MSH*, showing slower degradation kinetics but also singular sites of attack. Data at hand suggest that γ3-MSH of two species at least—human and barn owl—do share identical protection thanks to the polySer tails which, nonetheless, differ among each other significantly.[14] Also, adrenocorticotropic hormone (ACTH) displayed higher stability than α-MSH.[15] It may be conceivable that such mechanism of protection is independent from the exact nature of amino acids sequence/length, and therefore it can be applied to further peptide species. To this aim, we analyzed two couples of peptides: α-MSH with its precursor ACTH and neurotensin hormone ($NT_{1-13}$) with its precursor ($NT_{1-20}$) (Table 1). The latter example is for proof of principle investigation of the stabilizing mechanism since the natural C-terminal extension $NT_{1-20}$ has been shown to be active despite altering the signaling profile in cell-culture-based assays.[17] α-MSH/ACTH are very well-known hormones, deriving from POMC (Figure 1A),[18] as it is the case of γ2-MSH*/γ3-MSH. $NT_{1-13}$/$NT_{1-20}$ are endocrine peptides cut out from the neurotensin/neuromedin N precursor,[41] Along the same lines described above, the synthetic peptides were incubated in human plasma to monitor their degradation over time. Supernatants and pellets were treated separately. We found that both shorter peptides have reduced half-lives when compared with the longer analogues, and this is strikingly evident in the case α-MSH/ACTH (Figures 5 and 6). α-MSH peptide rapidly disappeared with estimated half-life of about 7.4 min and following a mechanism duplicate of that described for γ2-MSH*, indeed a progressive N-terminal processing is observed (Figure 5, Table 4). According to the expectations, ACTH did not undergo any attack at the N-terminus (Figure 5C), despite sharing 1 to 14 residues with α-MSH (Table 1). Of note, ACTH was extremely stable in human plasma (Figure 5), half-life resulting longer than 250 min. These data corroborated our hypothesis of a protection mechanism disconnected to the identity and length of the additional C-terminal stretch. Next, we focused our attention on a system unrelated to POMC. Similarly, we found that $NT_{1-13}$ was degraded at the N-terminus (Figure 6A,B; Table 5). $NT_{1-13}$ and $NT_{1-20}$ show a reduction to 50% of the starting amount of the full-length peptides at 6.8 and 11 min, respectively. In contrast, no fragments corresponding to aminopeptidase activity were detected in the case of the longer $NT_{1-20}$ (Figure 6A,B). The latter was rather attacked at the C-terminus, resulting in the release of multiple small C-terminal fragments. $NT_{1-13}$ and $NT_{1-20}$ shared only a mere cleavage product, generated by

**TABLE 4** Chemical characterization of ACTH peptide species isolated by RP-HPLC upon exposure to human plasma (Figure 5)

| | RT[a] (min) | Molecular mass (Da) | | Peptide species |
|---|---|---|---|---|
| | | Found[b] | Calculated[c] | |
| ACTH | 31.6 | 2,659.28 ± 0.07 | 2,659.00 | 14-37 |
| | 32.6 | 2,877.73 ± 0.49 | 2,878.24 | 15-39 |
| | | 2,343.86 ± 0.46 | 2,344.18 | 17-37 |
| | 40.1 | 1,807.97 ± 0.27 | 1,807.88 | 1-15 |
| | | 1,557.87 ± 0.06 | 1,557.79 | 3-15 |
| | | 1,429.53 ± 0.49 | 1,429.69 | 3-14 |
| | | 1,720.95 ± 0.26 | 1,720.85 | 2-15 |
| | 42.8 | 2,188.14 ± 0.43 | 2,188.08 | 18-37 |
| | | 980.55 ± 0.18 | 980.37 | 23-31 |
| | | 3,226.57 ± 0.39 | 3,226.69 | 9-37 |
| | 43.5 | 4,265.20 ± 0.42 | 4,264.84 | 1-37 |
| | 45.8 | 3,502.82 ± 0.01 | 3,502.98 | 9-39 |
| | | 4,540.98 ± 0.34 | 4,541.13 | 1-39 |
| | 46.4 | 2,464.18 ± 0.03 | 2,464.19 | 18-39 |
| | 47.0 | 2,211.18 ± 0.12 | 2,211.04 | 20-39 |
| | | 2,248.04 ± 1.00 | 2,248.18 | 1-18 |
| | | 2,317.39 ± 0.09 | 2,317.12 | 18-38 |
| | 47.4 | 1,983.91 ± 0.01 | 1,983.87 | 22-39 |
| α-MSH | 38.3 | 1,211.63 ± 0.01 | 1,211.62 | 5-14 |
| | 38.6 | 1,082.11 ± 0.01 | 1,082.58 | 6-14 |
| | 39.7 | 1,342.54 ± 0.03 | 1,342.66 | 4-14 |
| | 39.7 | 1,429.63 ± 0.05 | 1,429.69 | 3-14 |
| | 40.8 | 1,680.06 ± 0.02 | 1,679.79 | 1-14 |

Abbreviations: MSH, melanocyte stimulating hormone; RT, retention time; TCA, trichloroacetic acid.

[a]Peptides are listed in order of RT in RP-HPLC.

[b]Experimental molecular masses determined by ESI-QTOF-MS.

[c]Theoretical masses calculated on the base of the amino acid sequence.

**TABLE 5** Chemical characterization of NT peptide species isolated by RP-HPLC upon exposure to human plasma (Figure 6)

| | RT[a] (min) | Molecular mass (Da) | | Peptide species |
|---|---|---|---|---|
| | | Found[b] | Calculated[c] | |
| $NT_{1-20}$ | 26.2 | 383.14 ± 0.01 | 383.13 | 16-18 |
| | 30.6 | 344.15 ± 0.01 | 344.14 | 19-20 |
| | 34.5 | 1,029.57 ± 0.01 | 1,029.55 | 1-8p |
| | 36.1 | 709.33 ± 0.01 | 709.26 | 16-20 |
| | 39.6 | 1,800.18 ± 0.02 | 1,800.03 | 1-14p |
| | 40.0 | 2,664.74 ± 0.11 | 2,664.38 | 1-20 |
| | 41.2 | 2,647.82 ± 0.15 | 2,647.38 | 1-20p |
| | 43.3 | 1,672.19 ± 0.05 | 1,671.94 | 1-13p |
| $NT_{1-13}$ | 31.6 | 816.66 ± 0.01 | 816.50 | 8-13 |
| | 34.6 | 1,029.78 ± 0.01 | 1,029.55 | 1-8p |
| | 35.4 | 244.23 ± 0.01 | 244.18 | 12-13 |
| | 40.5 | 1,285.09 ± 0.11 | 1,284.73 | 4-13 |
| | 41.0 | 1,448.03 ± 0.18 | 1,447.79 | 3-13 |
| | 41.6 | 1,689.12 ± 0.14 | 1,688.94 | 1-13 |
| | 43.3 | 1,672.05 ± 0.12 | 1,671.94 | 1-13p |

*Note.* The letter p indicates the pyroglutamic form of the peptide.
Abbreviations: NT, neurotensin; RT, retention time.
[a]Peptides are listed in order of RT in RP-HPLC.
[b]Experimental molecular masses determined by ESI-QTOF-MS.
[c]Theoretical masses calculated on the base of the amino acid sequence.

processing at Arg8 (Table 5). Of note, a single stable peak of NTs (pNTs) was detectable, corresponding to the full-length peptides carrying a cyclized glutamic acid (pyroGlu, pGlu) at position 1. This phenomenon is very well described in literature as a spontaneous modification occurring to Glu residues.[42] As a proof-of-concept, the $pNT_{113}$ was almost stable over 90 min, confirming that the major route of degradation of the shorter hormone involved recognition at the N-terminus. On the contrary, the $pNT_{1-20}$ did decrease over time (estimated ~25%), in line with the hypothesis that the longer peptide is degraded starting from the C-terminus.

## 4 | CONCLUSIONS

In this study, we investigated the plasma degradation profile of three signaling peptides: γ2/γ3-MSH, α-MSH/ACTH hormones, both deriving from the pro-opimelanocortin (POMC) precursor, and $NT_{1-13}$/$NT_{1-20}$ neurotensin. C-terminal extensions present in the long forms (γ3-MSH, ACTH, and $NT_{1-20}$) of such hormones result beneficial to prolong the plasma-based half-life of peptides. Our study strongly supports the idea that length of peptide impacts on stability because it affects the peptide degradative pattern both in terms of kinetics and cleavage products profiles. Likely, the additional tail modulates the docking to specific serum proteins—enzymes or carriers/shielders—therefore regulating either the rate of conversion to products and/or the effective peptide bioavailability to degradation. It is the combination of the tail and specific plasma proteins that generates the "receipt" of a given peptide half-life. Our observations suggest that, along with other parameters, the consequences of extensions on the bioactivity of the drug has to be carefully evaluated. In particular, for the delivery of novel peptide drugs, an optimal design should consider, as a crucial step, the evaluation of the plasma degradation profile due to modifications added to the minimal active conserved sequence.

## ACKNOWLEDGEMENTS

This research was supported by Progetti di Ateneo-University of Padova 2017-N. C93C1800002600, MIUR-PNRA to P.P. (*Programma Nazionale Ricerche in Antartide*) (grant number PNRA18_00147), MIUR FFABR to L.C. (*Fondo di Finanziamento per le Attività Base di Ricerca*), the University of Lausanne to Prof. A.R. and Prof. Stefan Kunz†, and by the Swiss National Science Foundation grant number 31003A_153467 to Prof. A.R. The financial contribution from University of Padova and University of Lausanne for A.P. as Visiting Scientist is also gratefully acknowledged. We thank Silvia De Lorenzi and Giulia Zarantonello for help in the experiments and Dr Marino Bellini for technical assistance.

## CONFLICTS OF INTEREST

The authors declare no conflict of interest.

## ORCID

*Laura Cendron* https://orcid.org/0000-0002-0125-0461

## REFERENCES

1. Craik DJ, Fairlie DP, Liras S, Price D. The future of peptide-based drugs: peptides in drug development. *Chem Biol Drug Des*. 2013;81(1):136-147. https://doi.org/10.1111/cbdd.12055
2. Henninot A, Collins JC, Nuss JM. The current state of peptide drug discovery: back to the future? *J Med Chem*. 2018;61(4):1382-1414. https://doi.org/10.1021/acs.jmedchem.7b00318
3. Kaspar AA, Reichert JM. Future directions for peptide therapeutics development. *Drug Discov Today*. 2013;18(17–18):807-817. https://doi.org/10.1016/j.drudis.2013.05.011
4. Fosgerau K, Hoffmann T. Peptide therapeutics: current status and future directions. *Drug Discov Today*. 2015;20(1):122-128. https://doi.org/10.1016/j.drudis.2014.10.003
5. Sun L. Peptide-based drug development. *Mod Chem Appl*. 2013;1(1):1-2, e103. https://doi.org/10.4172/2329-6798.1000e103
6. Jenssen H, Aspmo SI. Serum stability of peptides. In *Peptide-Based Drug Design*, Vol. 494, Otvos L (ed). Humana Press: Totowa, NJ, 2008; 177–186, DOI: https://doi.org/10.1007/978-1-59745-419-3_10
7. Mathur D, Prakash S, Anand P, et al. PEPlife: a repository of the half-life of peptides. *Sci Rep*. 2016;6(1):36617. https://doi.org/10.1038/srep36617
8. Adessi C, Soto C. Converting a peptide into a drug: strategies to improve stability and bioavailability. *Curr Med Chem*. 2002;9(9):963-978. https://doi.org/10.2174/0929867024606731
9. Werle M, Bernkop-Schnürch A. Strategies to improve plasma half life time of peptide and protein drugs. *Amino Acids*. 2006;30(4):351-367. https://doi.org/10.1007/s00726-005-0289-3
10. Gentilucci L, De Marco R, Cerisoli L. Chemical modifications designed to improve peptide stability: incorporation of non-natural amino acids, pseudo-peptide bonds, and cyclization. *Current pharmaceutical*

*design*. 16(28) (2010): 3185-3203. http://www.eurekaselect.com/72674/article (accessed Sep 19, 2019).
11. Zhang L, Bulaj G. Converting peptides into drug leads by lipidation. *Curr Med Chem*. 2012;19(11):1602-1618. https://doi.org/10.2174/092986712799945003
12. Lau JL, Dunn MK. Therapeutic peptides: historical perspectives, current development trends, and future directions. *Bioorg Med Chem*. 2018;26(10):2700-2707. https://doi.org/10.1016/j.bmc.2017.06.052
13. Böttger R, Hoffmann R, Knappe D. Differential stability of therapeutic peptides with different proteolytic cleavage sites in blood, Plasma and Serum. *PLoS ONE*. 2017;12(6):e0178943. https://doi.org/10.1371/journal.pone.0178943
14. LöwK, Roulin A, Kunz S. A proopiomelanocortin-derived peptide sequence enhances plasma stability of peptide drugs. *FEBS Letters*. 2020. https://doi.org/10.1002/1873-3468.13855
15. Löw K, Ducrest A-L, San-Jose LM, et al. Molecular evolution of the pro-opiomelanocortin system in barn owl species. *PLoS ONE*. 2020 May 5;15(5):e0231163. https://doi.org/10.1371/journal.pone.0231163
16. Adan RAH, Gispen WH. Brain melanocortin receptors: from cloning to function. *Peptides*. 1997;18(8):1279-1287. https://doi.org/10.1016/S0196-9781(97)00078-8
17. Dores RM. Adrenocorticotropic hormone, melanocyte-stimulating hormone, and the melanocortin receptors: revisiting the work of Robert Schwyzer: a thirty-year retrospective. *Ann N Y Acad Sci*. 2009;1163(1):93-100. https://doi.org/10.1111/j.1749-6632.2009.04434.x
18. Cawley NX, Li Z, Loh YP. 60 YEARS OF POMC: biosynthesis, trafficking, and secretion of pro-opiomelanocortin-derived peptides. *J Mol Endocrinol*. 2016;56(4):T77-T97. https://doi.org/10.1530/JME-15-0323
19. Getting SJ, Kaneva M, Bhadresa Y, et al. Melanocortin peptide therapy for the treatment of arthritic pathologies. *Sci World J*. 2009;9:1394-1414. https://doi.org/10.1100/tsw.2009.163
20. Krude H, Biebermann H, Luck W, Horn R, Brabant G, Grüters A. Severe early-onset obesity, adrenal insufficiency and red hair pigmentation caused by POMC mutations in humans. *Nat Genet*. 1998;19(2):155-157. https://doi.org/10.1038/509
21. Loram LC, Culp ME, Connolly-Strong EC, Sturgill-Koszycki S. Melanocortin peptides: potential targets in systemic lupus erythematosus. *Inflammation*. 2015;38(1):260-271. https://doi.org/10.1007/s10753-014-0029-5
22. Hruby VJ, Cai M, Cain JP, Mayorov AV, Dedek MM, Trivedi D. Design, synthesis and biological evaluation of ligands selective for the melanocortin-3 receptor. *Curr Top Med Chem*. 2007;7(11):1107-1119. https://doi.org/10.2174/156802607780906645
23. Gill SC, von Hippel PH. Calculation of protein extinction coefficients from amino acid sequence data. *Anal Biochem*. 1989;182(2):319-326. https://doi.org/10.1016/0003-2697(89)90602-7
24. Suda H, Aoyagi T, Takeuchi T, Umezawa H. A thermolysin inhibitor produced by actinomycetes: phosphoramidon. *J Antibiot (Tokyo)*. 1973;26(10):621-623. https://doi.org/10.7164/antibiotics.26.621
25. Komada Y, Peiper S, Tarnowski B, Melvin S, Kamiya H, Sakurai M. Shedding of the common acute lymphoblastic leukemia antigen (CALLA) by lymphoblastoid cell lines. *Leuk Res*. 1986;10(6):665-670. https://doi.org/10.1016/0145-2126(86)90270-5
26. Bayés-Genís A, Barallat J, Galán A, et al. Soluble neprilysin is predictive of cardiovascular death and heart failure hospitalization in heart failure patients. *J Am Coll Cardiol*. 2015;65(7):657-665. https://doi.org/10.1016/j.jacc.2014.11.048
27. Kenny AJ, Bourne A, Ingram J. Hydrolysis of human and pig brain natriuretic peptides, urodilatin, C-type natriuretic peptide and some C-receptor ligands by endopeptidase-24.11. *Biochem J*. 1993;291(1):83-88. https://doi.org/10.1042/bj2910083
28. Takaki Y, Iwata N, Tsubuki S, et al. Biochemical identification of the neutral endopeptidase family member responsible for the catabolism of amyloid peptide in the brain. *J Biochem (Tokyo)*. 2000;128(6):897-902. https://doi.org/10.1093/oxfordjournals.jbchem.a022839
29. Solomon SD, Rizkala AR, Gong J, et al. Angiotensin receptor neprilysin inhibition in heart failure with preserved ejection fraction. *JACC Heart Fail*. 2017;5(7):471-482. https://doi.org/10.1016/j.jchf.2017.04.013
30. Kathpalia PP, Charlton C, Rajagopal M, Pao AC. The natriuretic mechanism of gamma-melanocyte-stimulating hormone. *Peptides*. 2011;32(5):1068-1072. https://doi.org/10.1016/j.peptides.2011.02.006
31. Keil B. *Specificity of Proteolysis*. Springer Berlin Heidelberg: Berlin, Heidelberg, 1992, DOI: https://doi.org/10.1007/978-3-642-48380-6
32. Ingrosso D, Fowler AV, Bleibaum J, Clarke S. Specificity of endoproteinase asp-N (Pseudomonas fragi): cleavage at glutamyl residues in two proteins. *Biochem Biophys Res Commun*. 1989;162(3):1528-1534. https://doi.org/10.1016/0006-291X(89)90848-6
33. Drapeau GR, Boily Y, Houmard J. Purification and properties of an extracellular protease of Staphylococcus aureus. *J Biol Chem*. 1972;247(20):6720-6726.
34. Fontana A, de Laureto PP, Spolaore B, Frare E, Picotti P, Zambonin M. Probing protein structure by limited proteolysis. *Acta Biochim Pol*. 2004;51(2):299-321. https://doi.org/10.18388/abp.2004_3573
35. Jia Y, Kim J-H, Nam B, et al. The dipeptide H-Trp-Glu-OH (WE) shows agonistic activity to peroxisome proliferator-activated protein-α and reduces hepatic lipid accumulation in lipid-loaded H4IIE cells. *Bioorg Med Chem Lett*. 2014;24(13):2957-2962. https://doi.org/10.1016/j.bmcl.2014.04.019
36. Jia Y, Kim J-H, Nam B, et al. The dipeptide H-Trp-Arg-OH (WR) is a PPARα agonist and reduces hepatic lipid accumulation in lipid-loaded H4IIE cells. *Appl Biochem Biotechnol*. 2015;175(2):1211-1220. https://doi.org/10.1007/s12010-014-1302-7
37. Oliva R, Falcigno L, DAuria G, et al. Structural investigation of the HIV-1 envelope glycoprotein Gp160 cleavage site, 2: relevance of an N-terminal helix. *Chembiochem Eur J Chem Biol*. 2003;4(8):727-733. https://doi.org/10.1002/cbic.200200541
38. Hubbard SJ, Eisenmenger F, Thornton JM. Modeling studies of the change in conformation required for cleavage of limited proteolytic sites. *Protein Sci Publ Protein Soc*. 1994;3(5):757-768. https://doi.org/10.1002/pro.5560030505
39. Marcelino AMC, Gierasch LM. Roles of beta-turns in protein folding: from peptide models to protein engineering. *Biopolymers*. 2008;89(5):380-391. https://doi.org/10.1002/bip.20960
40. Grieco P, Balse PM, Weinberg D, MacNeil T, Hruby VJ. D-amino acid scan of gamma-melanocyte-stimulating hormone: importance of Trp (8) on human MC3 receptor selectivity. *J Med Chem*. 2000;43(26):4998-5002. https://doi.org/10.1021/jm000211e
41. Dobner PR, Barber DL, Villa-Komaroff L, McKiernan C. Cloning and sequence analysis of CDNA for the canine neurotensin/neuromedin N precursor. *Proc Natl Acad Sci*. 1987;84(10):3516-3520. https://doi.org/10.1073/pnas.84.10.3516
42. Beck A, Bussat M-C, Klinguer-Hamour C, et al. Stability and CTL activity of N-terminal glutamic acid containing peptides. *J Pept Res*. 2001;57(6):528-538. https://doi.org/10.1034/j.1399-3011.2001.00895.x

## SUPPORTING INFORMATION

Additional supporting information may be found online in the Supporting Information section at the end of this article.

**How to cite this article:** Palazzi L, Pasquato A, Vicario M, Roulin A, Polverino de Laureto P, Cendron L. C-terminal tails mimicking bioactive intermediates cause different plasma degradation patterns and kinetics in neuropeptides γ-MSH, α-MSH, and neurotensin. *J Pep Sci*. 2020;e3279. https://doi.org/10.1002/psc.3279